Assignment 1 report

Team n. 11

Students:

Bontempelli Elia, n. 233225
Cavalaglio Alessandro, n. 232889
Scarperi Davide, n. 231603

ACADEMIC YEAR 2022/2023

Contents

1 Introduction

In this first part of the project, it is requested to fit the MF96 tyre model coefficients on a dataset of measured tyre forces for a F-SAE tyre (Hoosier 18.0 x 6.0 - 10 R25B). This means that the pure longitudinal force, the pure lateral force, the combined behaviour and the self-aligning moment must be computed through the Pacejka's Magic Formula.

Firstly it has been used Maple to generate the MATLAB functions essential for the calculation of forces and moment; then the main code has been developed in MATLAB.

The sign convention used for forces, moment and wheel slip is the adapted SAE reference, used also in Pacejka's book.

It has been noticed, that for low values of vertical load F_z some noise was present in the results and for this reason it has been chosen $Fz = 900N$, throughout the project since it was the value for which the theoretical results best matched the experimental data.

The problem of tyre data fitting comes down to the optimization of the coefficients of the Magic Formula. A least-squares approach is used to find the optimal parameters that minimize the squares of the residuals between the fitted function and real data. This problem is a constrained minimization, which can be solved in MATLAB with the function $fmincon$.

In order to understand the validity of the optimization performed, for each case considered, plots with raw data and fitting are reported. In addition, for a more complete analysis, to have a numerical confirmation of the results obtained, performance index for each fitting are computed; in particular it has been considered R-squared index and, in the cases where R-squared was low, the root mean square error (RMSE) to have a counter proof.

2 Longitudinal force

In the first phase it has been computed the longitudinal force applied to the tyre in order to fit the experimental data. The pure longitudinal force (side slip equal to 0) fitted under different settings is displayed in the pictures below by optimisation of the Pacejka's Magic Formula coefficients.

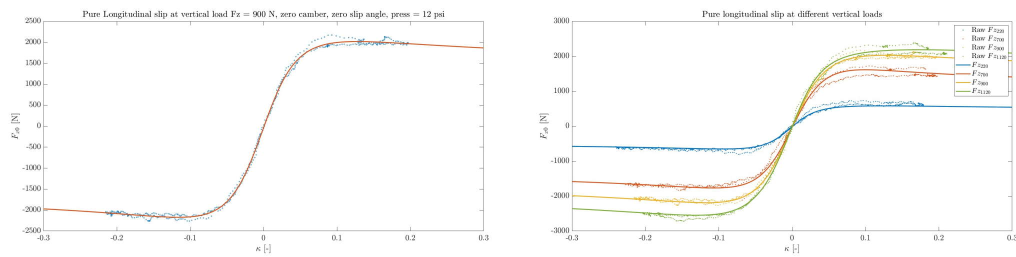

(a) Case with fixed vertical load (b) Case with variable vertical load

Figure 1: Pure longitudinal force with fixed camber

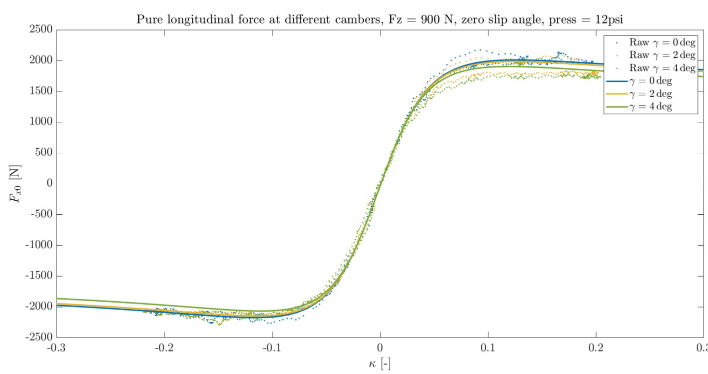

Figure 2: Pure longitudinal force with fixed vertical load and variable camber

Then, also the combined behaviour (when both longitudinal and side slip are not 0) has been investigated and fit. The results are reported in the following Figure.

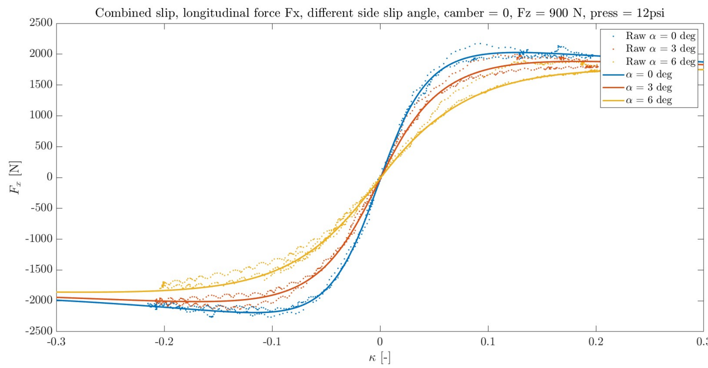

Figure 3: Combined longitudinal force with fixed vertical load, fixed camber and variable side slip

The optimized parameters found from the longitudinal force fitting are shown in the following table.

pCx1	**pDx1**	**pEx1**	**pEx4**	**pKx1**	**pHx1**	**pVx1**
1.484	2.358	0.149	-0.808	53.982	9.585e-04	-0.091
pDx2	**pEx2**	**pEx3**	**pKx2**	**pKx3**	**pHx2**	**pVx2**
-0.593	1.512	2.235	-0.052	0.533	4.301e-05	0.096
pDx3						
10.36						
rBx1	**rBx2**	**rCx1**	**rHx1**			
10.141	13.489	1.211	-0.027			

Table 1: Optimized longitudinal parameters

	Fx0	**Fx0 varFz**	**Fx0 varGamma**	**Fx comb**
R-squared	0.999	0.726	0.998	0.961
RMSE		85.079		

Table 2: Indexes of performance for the longitudinal force

3 Lateral force

The same analysis were done for the lateral force, which has been computed both in pure and combined state. Also in this case, the MF96 coefficients fit perfectly the data collected from the tyres, as it is shown in the following figures.

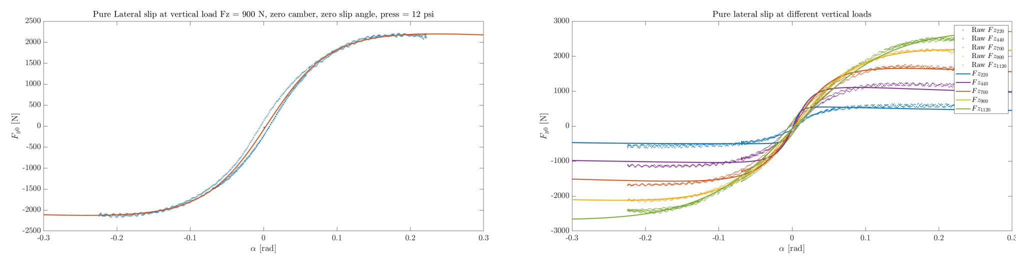

(a) Case with fixed vertical load (b) Case with variable vertical load

Figure 4: Pure lateral force with fixed camber

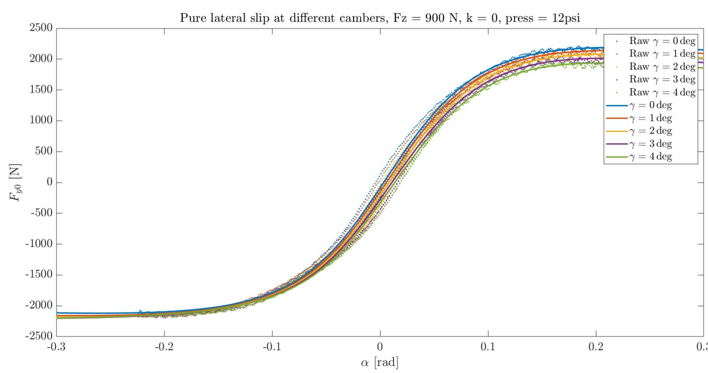

Figure 5: Pure lateral force with fixed vertical load and variable camber

Since there are only a few discrete values of side slip angle in the dataset, it was necessary to change the approach for the combined lateral force. In fact, we optimized the coefficients using the combined lateral force for only the three values of side slip angle that were available.

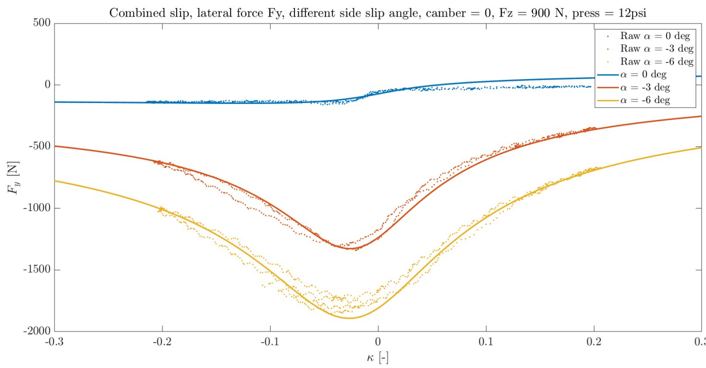

Figure 6: Combined lateral force with fixed vertical load, fixed camber and variable side slip

The optimized parameters found from the longitudinal force fitting are shown in the following table.

pCy1	**pDy1**	**pEy1**	**pHy1**	**pKy1**	**pKy2**	**pVy1**		
1.637	2.402	0.478	-0.005	-60.291	-0.259	0.040		
pDy2	**pEy2**	**pHy2**	**pVy2**					
0.017	-0.613	-0.003	-0.072					
pDy3	**pEy3**	**pEy4**	**pHy3**	**pKy3**	**pVy3**	**pVy4**		
7.134	0.322	-9.875	-0.045	0.995	-2.841	-0.997		
rBy1	**rBy2**	**rBy3**	**rCy1**	**rHy1**	**rVy1**	**rVy4**	**rVy5**	**rVy6**
16.491	28.617	-0.068	0.945	0.021	-0.143	0.601	-0.243	21.329

Table 3: Optimized lateral parameters

	Fy0	**Fy0 varFz**	**Fy0 varGamma**	**Fy comb**
R-squared	0.998	0.830	0.994	0.514
RMSE		95.105		53.908

Table 4: Indexes of performance for the lateral force

4 Self-aligning moment

Finally, the self-aligning moment generated by the lateral force on the tyre has been determined and fit with the test data with positive results in two cases, which are with fixed and variable vertical load.

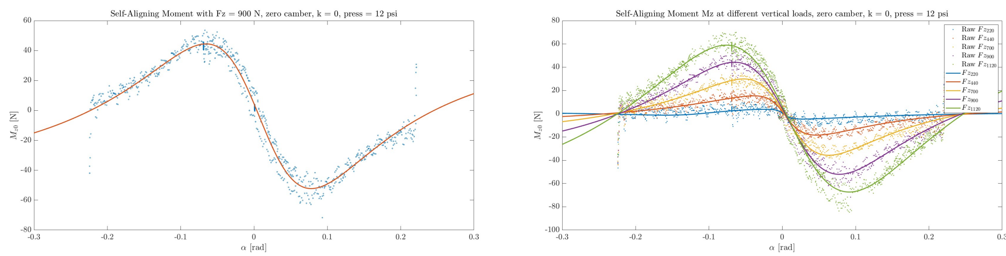

(a) Case with fixed vertical load (b) Case with variable vertical load

Figure 7: Self-aligning moment

qBz1	**qBz9**	**qBz10**	**qCz1**	**qDz1**	**qDz2**	**qDz6**	**qEz1**	**qEz4**	**qHz1**
7.416	4.121	3.988	1.675	0.196	0.058	0.003	0.543	0.022	-0.012
qBz2	**qBz3**	**qDz7**	**qEz2**	**qEz3**	**qHz2**				
-1.145	-4.254	0.003	-0.297	-0.647	-0.003				

Table 5: Optimized self-aligning moment parameters

	Mz0	**Mz0 varFz**
R-squared	0.967	0.543
RMSE		4.479

Table 6: Indexes of performance for the self-aligning moment

5 Final considerations

The most challenging aspect of the assignment was finding the beginning values and the bounds to do the optimization, since in absence of reference thresholds, erroneous values were frequently picked and this caused occasional fails in the optimization.

Performing several number of simulations gives us the possibility to understand better which parameters had more influence on the computation of the force and thus we paid more attention on the tuning of the initial values and the boundaries for these parameters. While we were gradually moving towards the best fitting solution, we gradually narrowed the margins in order to focus the search of the optimal solution in a smaller interval of values.

As can be shown visually in the plots and by the performance indices, the optimization performed led to coefficients that suit very well the experimental data.